Analysis of a model for anomalous diffusion behavior of CO_2 in the macromolecular network structure of coal and its significance for CO_2 sequestration

Saikat Mazumder, SPE, Shell Exploration and Production; **Fred Vermolen**, SPE and **Johannes Bruining**, SPE, Delft University of Technology

Summary

This paper gives an analysis of the Thomas and Windle model, to determine its usefulness for describing anomalous diffusion of CO_2 in coal and its relation to matrix swelling. In addition a Finite Element description for this model is derived. For reasons of easy reference a shortened derivation of the Thomas and Windle model is presented, which was originally derived to describe diffusion in polymers. The derivation includes the surface saturation effects proposed by Hui. As the cumulative sorption showed t^{α} behavior with $\alpha>0.5$, the behavior was described as enhanced diffusion or even superdiffusion. Analysis of the model equation shows no evidence for super-diffusion even if non-Fickian behavior is observed, i.e., there is (1) an initial phase in which the coal surface gets saturated with a slope > 0.5 in a log-log plot of cumulative sorption versus time, (2) an intermediate phase that shows the typical square root of time behavior of an ordinary diffusion process, (3) a final phase with a slope < 0.5 towards equilibrium. The cumulative mass is for all times less than would have been obtained for pure diffusion in a particle characterized by a rubber diffusion coefficient. The slow saturation at the surface masks a process where fast stress induced diffusion dominates, which can indeed be faster than Fickian. The cumulative sorption rates give similar behavior as the Rückenstein model, but the advantage of the Thomas and Windle model is that it can also calculate the resulting coal swelling effects.

Introduction

Stress induced diffusion plays an important part in many engineering applications, such as polymer sciences, biomedical applications and possibly in diffusion processes in hydrates. It is of interest to investigate its importance in CO_2 penetration and simultaneous induced swelling of coal in carbon sequestration applications. The "swelling" of coal by a penetrant is caused by an increase in the volume occupied by the coal as a result of the viscoelastic relaxation of its highly crosslinked macromolecular structure.

The idea that CO_2 penetration in coal has some similar features as sorbent penetration in glassy polymers is not new.

Indeed, the similarities in structure between coal and glassy polymers have led to the perception (Ritger and Peppas 1987-a, 1987-b) that CO_2 penetration has many analogous features that are observed for organic sorbents penetrating into glassy polymers. Ritger et al. propose the application of theories of sorption behavior of polymers to coals. During penetrant transport at low or moderate temperatures into the macromolecular network of coal, the network density decreases. (Ritger and Peppas 1987-a, 1987-b). Therefore, it is asserted that an increase of the penetrant volume fraction of the network can be viewed as an effective decrease of the glass transition temperature (Hsieh et al. 1987). Structural changes induced during this process include swelling, microcavity formation and a primary phase transition requiring rearrangements of chain segments. Such changes are dominated by relaxational phenomena.

There is a vast literature describing penetration of organic molecules or CO_2 in coal with evidence that the macromolecular structure changes during the sorption process involving a glassy and rubbery structure of coal. A selected number of papers summarize these ideas.

For example Nirzaeian and Hall (2006) present experimental results using differential scanning and find that CO_2 causes significant plasiticization effects and changes in the macro-molecular structure. Goodman et al. (2000) use reflectance infrared spectroscopy to show that the diffusion coefficient increases on second exposure, indicating that CO_2 causes structural changes. Cody et al. (1993) present a simple model of an entangled macromolecular network. To this network several properties are assigned such as a cooperative diffusion coefficient (10^{-9} -10^{-10} m^2/s) and a coefficient of viscosity in the range 10^{11}-10^{13} P. Moreover they observe a relaxation effect in the frequency range or 10^{-3} Hz.

Karacan (2003) discusses sorption and swelling in a confined and stressed coal during CO_2 injection". They use X-ray computed tomography to observe swelling and "de-swelling" with characteristic times between 5000-7000 minutes. Experiments are explained by assuming a polymeric structure. Krzesiński (2001-a, b) measures the effects of solvents on the elastic properties of coal. They consider a polymeric coal model where aromatic clusters of graphite like structures are connected by aliphatic chains. The elastic modulus increases with increased cross-linking of the polymeric structure. It is concluded that the dependence of the elastic modulus on swelling exhibits the same nature as that for polymers. Elastic moduli are characteristic for polymers in the glassy state, e.g., 5.19 GPa for bituminous coal about 10000 times as large as for polymers in the rubbery state.

Also in the Dietz laboratory, one of the authors of this paper, observed a correlation between CO_2 sorption and strain effects (Mazumder and Wolf 2008). Comparison between Figures 2-6 with Figures 7-11 in Mazumder &Wolf (2008) shows that sorption of CO_2 is strongly correlated with the observed strain, where the conversion between displaced volume and time can be found in Tables 3-4.

There is also field evidence of the coupling between sorption

and swelling. In The RECOPOL project in Poland problems with injectivity were attributed to coal swelling as a consequence of CO_2 sorption (Pagnier et al. 2003; Nady 2006, Shi and Durucan 2004).

For the ease of reference we summarize here below the description of Ritger and Peppas (1987-a, 1987-b), who show the relevance of case II diffusion for coal. It is convenient to describe the mass uptake by an empirical equation

$$\frac{M_t}{M_e} = k_1\sqrt{t} + k_2 t \approx kt^n, \quad (1)$$

where M_t is the mass uptake at time t and M_e is the equilibrium mass uptake, k is a constant incorporating characteristics of the macromolecular network system and the penetrant, and n is the diffusional exponent. Fickian diffusion and "Case II transport" for a thin slab are defined by n equal to 0.5 and n equal to 1 respectively. An operational definition for anomalous transport behavior is any diffusion like process that is intermediate between Fickian and Case II, and has a value of n between 0.5 and 1. Such an operational definition may be deceiving as case II diffusion has a connotation with faster than Fickean, but by its definition it includes delayed surface saturation effects. In spite of this, it is often stated that the diffusion of a penetrant into glassy polymers varies between two extremes. If the diffusion is controlled by the volume fraction gradient between the centre and the outside of the coal matrix, the diffusion mechanism is Fickian. If the transport is controlled by a stress gradient induced by the penetration of molecules, the diffusion mechanism is anomalous. Vrentas et al.[3, 4] introduced the Deborah number (D_e) as a means of characterizing penetrant uptake. In terms of D_e, the nature of the sorption process can be distinguished by the ratio of two characteristic times, namely a structural relaxation time λ and a characteristic diffusion time, θ. The Deborah number is written as,

$$D_e = \frac{\lambda}{\theta}. \quad (2)$$

For $D_e \gg 1$, i.e. relaxation time much larger than diffusion time, there is effectively no time variation of the macromolecular structure during the diffusion process. Such a sorption process can be described by Fickian diffusion. For $D_e \ll 1$, i.e., a relaxation time much smaller than diffusion time, conformational changes in the macromolecular structure occur instantaneously with respect to the time scale of diffusion. In this case the transport process is also described by Fickian diffusion. Hence, in relation to the diffusional exponent n, systems exhibiting $D_e \gg 1$ or $D_e \ll 1$ can be characterized by n equal to 0.5 (for slab geometry). When D_e = O(1), i.e., the relaxation and diffusion times are of the same order of magnitude, case II diffusion would become relevant.

The characteristic diffusion time of a thin slab of length l surrounded by the penetrant would be $\theta = 4l^2/D$, where D is the diffusion coefficient. Substitution into Eq. (2) leads to

$$D_e = \frac{4\lambda D}{l^2}. \quad (3)$$

Assuming l to mean the distance of penetration into the coal the following behavior is observed. Initially the behavior would be Fickian, but this behavior is not observed, as there is a time lag before the surface gets saturated with the penetrant (see below). Subsequently there will be a period where the behavior is Non-Fickian. Then in the long term the behavior will again be Fickian unless the matrix block is too small to reach this situation.

There is a large amount of literature on anomalous diffusion, which already dates back to the sixties. Alfrey et al.[5] have presented a second limiting case for sorption, where the rate of transport is entirely controlled by molecular relaxation. This type of transport mechanism is designated as Case II transport. Thomas and Windle (1982) proposed that the rate-controlling step at the penetrant front is the time dependent mechanical deformation of the glassy polymer in response to the thermodynamic swelling stress. The T&W model stimulated experimental research of Case II sorption, particularly by Lasky et al. (1988) and Gall et al. (1991) on a number of polymer / sorbent systems using the Rutherford backscattering technique. Hui et al. (1987a, 1987b) dealt with both the initial transient penetration of the sorbent and the final steady state motion of the sorption front - all within the framework of the T&W model. The advantage of the T&W model described by Hui et al. (1987a, 1987b) is that it is almost entirely based on the fundamental laws of physics including a clear derivation of the model equations (see Fig. 1). There have been a number of other model developments, e.g., Govindjee et al. (1993) that emphasize the importance of thermodynamic driving forces and a glass to rubber transition.

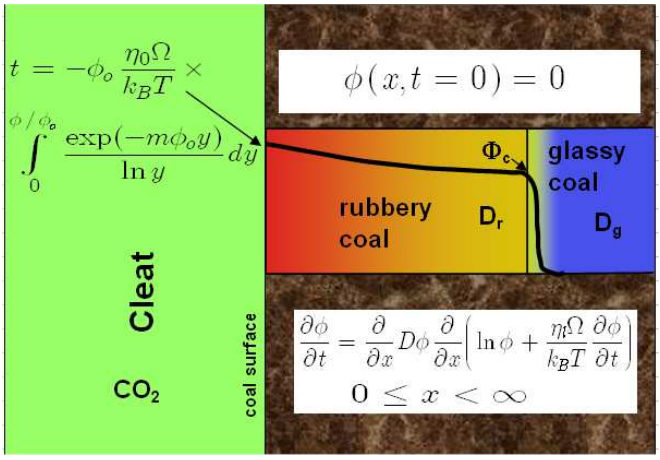

Fig. 1 *Volume fraction profile for Case II sorption into an infinite sheet with a Fickian diffusion front preceding the advancing boundary between swollen (called rubbery) and the essentially unpenetrated glassy coal. The volume fraction of CO_2 in the coal is denoted by ϕ.*

Durning[12] extended the T&W model using irreversible thermodynamics. They replaced the viscous model with the Maxwell viscoelastic model, so that a relaxation time can be defined. The relation between osmotic pressure and the stresses on the coal was analyzed using the force balance. Argon et al. (1999) presented a mechanistic model, which considers the conditions that govern the self-similar

propagation of fully developed Case II sorption fronts, combined with their Fickian precursors.

The characteristics of Case II diffusion in coal are usually described as follows (see Fig. 1):
(a) The penetrant advances through the coal and simultaneously converts the glassy structure to a more rubber like (swollen) structure. There will be a short glass-rubber transition zone. Far downstream the penetrant volume fraction is zero. Upstream the rubber zone the penetrant is at equilibrium volume fraction. The rubber part is substantially swollen with respect to the glassy part.
(b) After some initializing effects a semi-steady state occurs, where a given volume fraction profile travels through the slab more or less proportional to time
(c) The swollen matrix behind the advancing front is at a uniform state of swelling.

The question arises whether the description given above is also supported by the model equations of T&W clarified by Hui. Therefore the authors of this paper reviewed the modeling both from the physical as from the mathematical point of view. This entails a shortened derivation of the equation originally derived by (Thomas et al. 1982) and rederived by Hui et al. (1987a, 1987b) with an emphasis on extended irreversible thermodynamics (Jou et al. 2001). Extended irreversible thermodynamics (EIT) differs from classical irreversible thermodynamics (CIT) by not only characterizing a volume element by thermodynamic variables (temperature, pressure, volume fraction), but also by its gradients.

The mathematical analysis of the model is based on a dimensional analysis and a solution of the long-term behavior, using an analytical solution proposed by Sherwood and Pigford (Bird et al. 2002), which deals with an analytical solution that includes a sudden jump in diffusion coefficients. A linearized version of the model of the model is included.
The current literature on case II diffusion for polymers cannot be directly used for comparison to measured data because the numerical schemes proposed at the time (1982-1987) are very unconventional and are now replaced by more accurate methods. Due to the unconventional form of the model equations, it was necessary to perform an analysis of the existence and uniqueness of the solutions (Mikelic and Bruining (2008)). The authors of this paper include a full description of an improved numerical scheme in the appendix of this paper. The numerical solution is used to validate whether the T&W model indeed shows anomalous (super) diffusion behavior.

Derivation of the equations

The salient features of the T&W model are well summarized by Hui et al. (1987a, 1987b). For the ease of reference a shortened derivation is included that stresses the use of Extended Irreversible Thermodynamics and hence the fundamental nature of the model development. According to the T&W model, the volume fraction ϕ of the penetrant is a function of the spatial dimension x, and time t, i.e. $\phi = \phi(x,t)$.

The increase in the volume fraction occurs by the penetrant molecules occupying "interstitial" sites between polymer chains in the coal. To a good approximation the glassy coal is a random close-packed arrangement of chain segments with little "free volume". There are only a limited number of such sites that may be occupied without the concurrent motion of the cross-links. If the equilibrium volume fraction of penetrant is larger than the volume fraction of the existing interstitial sites, there is a geometric problem associated with the sorption. As compared to the glassy state of coal, in the rubbery state the crosslink polymeric chains can move separately and rapidly by a process involving rotation of main chain bonds so that the equilibrium is obtained almost instantaneously. Thus, the initial penetrant volume ϕ will be less than the equilibrium volume fraction ϕ_0. The volume fraction ϕ approaches this value only as permitted by the motion of the polymeric chains in coal.
Thomas et al.[6] treat the swelling rate, or the rate of change of volume fraction of penetrant, as the rate of linear viscous creep deformation driven by the osmotic stress, P_{xx}. The amount of penetrant is expressed in terms of the volume fraction ϕ, which is related to the volume fraction by $\phi = c/\Omega$, where Ω is the partial molecular volume.
The derivation included here is based on the article by Hui et al. (1987a, 1987b) and Landau and Lifschitz (1975), i.e. the molar flux J is not only driven by the volume fraction gradient $\partial\phi/\partial x$, but also by the stress gradient, $\partial P_{xx}/\partial x$ i.e.,

$$J = -D\phi\frac{\partial}{\partial x}\left(\ln\phi + \frac{\Omega}{k_B T}P_{xx}\right). \tag{4}$$

The coefficients are determined by comparison to CIT. P_{xx} is interpreted as the stress that balances the osmotic pressure.
In addition Extended Irreversible Thermodynamics (Jou et al. 2001) is applied to show that vice-versa also the stress is related to molar flux gradient as

$$P_{xx} = -\eta_l\frac{\partial J}{\partial x} = \eta_l\frac{\partial\phi}{\partial t}, \tag{5}$$

where η_l is the elongational viscosity. The elongational viscosity is introduced here to describe the interaction between the penetrant molecule (e.g., CO_2) and the polymer (e.g., coal) and is not a bulk property of the polymer. The second equation follows from the mass balance equation

$$\frac{\partial\phi}{\partial t} + \frac{\partial J}{\partial x} = 0. \tag{6}$$

The diffusion coefficient depends on the volume fraction. Below a critical volume fraction ϕ_c a diffusion coefficient D_g characteristic of a glassy state is used, and above ϕ_c the diffusion coefficient D_r characteristic of the rubber (swollen) state is used. It can be expected that $D_r / D_g >> 1$. In the model an abrupt change of the diffusion coefficients at ϕ_c is used, and D_r and D_g are considered constant for $\phi > \phi_c$ and $\phi < \phi_c$ respectively.
Therefore substitution of Eq. (5) into Eq. (4) leads to,

$$J = -D\frac{\partial}{\partial x}\left(\phi + \frac{\eta_l \Omega \phi}{k_B T}\frac{\partial \phi}{\partial t}\right), \quad (7)$$

and after substituting into the mass balance equation, Eq. (6), one arrives at

$$\frac{\partial \phi}{\partial t} = \frac{\partial}{\partial x}\left(D\phi\frac{\partial}{\partial x}\left(\ln\phi + \frac{\eta_l \Omega}{k_B T}\frac{\partial \phi}{\partial t}\right)\right). \quad (8)$$

Sorption effects, leading to retardation can also be formally included in a slower diffusion coefficient *D*. As the diffusion coefficient for surface diffusion is essentially an unknown parameter we did not include sorption effects separately. The elongational viscosity η_l is supposed to depend on the volume fraction of the penetrant as

$$\eta_l = \eta_o \exp(-m\phi), \quad (9)$$

where m is a material constant and η_0 is the volumetric viscosity of the un-swollen coal sample. The final equilibrium volume fraction is reached when the coal has swollen to make the stress P_{xx} equal to zero. In this case the volume fraction of CO_2 in the coal is in equilibrium with the CO_2 in the fluid phase outside the coal. Also the CO_2 in the stressed coal is in equilibrium with the CO_2 in the fluid phase. The change in chemical potential $d\mu = \Omega dP_{xx} + k_B T d\ln\phi$. Equating the chemical potential in the unstressed ($P_{xx}^{(0)} = 0$) and stressed state leads to:

$$\Omega P_{xx} + k_B T \ln\phi = \Omega P_{xx}^0 + k_B T \ln\phi_o \quad (10)$$

Substitution of Eq. (5) and Eq. (9) into Eq. (10) leads to

$$\ln\phi/\phi_o = -\frac{\eta_0 \Omega}{k_B T}\exp(-m\phi)\frac{d\phi}{dt}. \quad (11)$$

The solution of this equation is (see Hui et al. (1987a, 1987b)

$$t = -\phi_o \frac{\eta_0 \Omega}{k_B T}\int_0^{\phi/\phi_o}\frac{\exp(-m\phi_o y)}{\ln y}dy, \quad (12)$$

which uses the boundary condition that ϕ =0 at *t=0*.

The T&W model can be extended by including a relaxation term in the model equations (Jou 2001).

Analytical considerations for the Case II diffusion problem

Boundary conditions

At $x = 0$ the volume fraction is given by $\phi(x = 0, t) = \phi_g(t)$, which is given by Eq. (12). At $x = L$ there is a no flow boundary condition in our numerical code, i.e.,

$$D\frac{\partial \phi}{\partial x} + \frac{1}{B}D\phi\frac{\partial}{\partial x}\left(\exp(-m\phi)\frac{\partial \phi}{\partial t}\right) = 0,$$

which can be rewritten as

$$D\frac{\partial \phi}{\partial x} + \frac{1}{B}D\phi\frac{\partial}{\partial t}\left(\exp(-m\phi)\frac{\partial \phi}{\partial x}\right) = 0 \ .$$

The equation is satisfied when $\frac{\partial \phi}{\partial x} = 0$ at $x = L$. The initial conditions are ϕ(x,t=0) =0 and $\partial\phi$(x,t=0)/ ∂t =0.

Dimensionless form

Eq. (6) can be rescaled using $D_g t / L^2 \to t$, $D / D_g \to D$, $x / L \to x$ to obtain

$$\frac{\partial}{\partial t}\phi = \frac{\partial}{\partial x}\left(D\frac{\partial}{\partial x}\phi\right) + \beta\frac{\partial}{\partial x}\left(D\phi\frac{\partial}{\partial x}\exp(-m\phi)\frac{\partial}{\partial t}\phi\right), \quad (13a)$$

where $\beta = \Omega D_g \eta_o / (k_B T L^2)$, showing that for long time, i.e., large sample length L, or penetration depth, the relaxation term becomes negligible. For the parameters used in the table it follows that $\beta = 3.5 \times 10^{-5} / L^2$. It is therefore to be expected that the significance of the third term strongly depends on the elongational viscosity (see Eq. (9)), the diffusion coefficient and the size of the coal particle in which the penetration occurs. Neglecting the relaxation term allows an analytical solution, which shows $\sqrt{t}$ behavior as can be shown by the Sherwood-Pigford model (see below).

The dimensionless boundary conditions at *x=0* reads

$$t = -\phi_o \beta \int_0^{\phi/\phi_o}\frac{\exp(-m\phi_o y)}{\ln y}dy, \quad (13b)$$

The T&W model equations are thus formulated with three parameters, viz., the interaction parameter β, the material constant *m*, and the ratio of the diffusion coefficients *D*. The value of the glass diffusion coefficient D_g only acts as a time scaling parameter.

Sherwood and Pigford approach

Consider a diffusion problem, where the diffusion coefficient assumes different but constant values below and above a critical concentration c_s. A similar problem has been solved by Sherwood and Pigford as explained in the new book of Bird's transport phenomena (Bird et al. 2002). Here c(x,t) replaces ϕ(x,t) to adopt the notation in Bird et al. (2002).

$$\frac{\partial c}{\partial t} = \frac{\partial}{\partial x}\left(D(x)\frac{\partial c}{\partial x}\right), \qquad x > 0, \ t > 0,$$

where

$$D(x) = \begin{cases} D_r & , \quad \text{for} \quad x < s(t), \\ D_g & , \quad \text{for} \quad x \geq s(t), \end{cases}$$

in which s(t) denotes the interface position. Again D_r is used to denote the diffusion coefficient in the rubber state, whereas D_g is the diffusion coefficient in the glass state.

The problem is subjected to the following boundary and initial conditions

$$\begin{aligned} c(0,t) &= c_0 \quad , \quad t>0 \\ \lim_{x\to\infty} c(x,t) &= 0 \quad , \quad t>0 \\ c(x,0) &= 0 \quad , \quad x>0 \\ s(0) &= 0 \quad , \quad x>0 \end{aligned} \tag{14}$$

where $x=s(t)$ denotes the interface position.
Moreover there will be continuity of flux and concentration at the interface, i.e.,

$$\begin{aligned} D_r \frac{\partial c}{\partial x}(s(t)_-,t) &= D_g \frac{\partial c}{\partial x}(s(t)_+,t) \quad \text{on } s(t) \quad t>0 \\ c(s(t)_-,t) &= c(s(t)_+,t) \quad \text{on } s(t) \quad t>0 \end{aligned}$$

It can be expected that the solutions are of the type

$$c(x,t) = \begin{cases} c_0 + C_2 \operatorname{erf}\frac{x}{\sqrt{4D_R t}} & \text{for} \quad 0 < x \le s(t) \\ C_3 - C_3 \operatorname{erf}\frac{x}{\sqrt{4D_L t}} & \text{for} \quad s(t) < x < \infty \end{cases} , \tag{15}$$

using the boundary conditions in (14).
Continuity of concentration gives

$$\begin{aligned} c_0 + C_2 \operatorname{erf}\frac{s(t)}{\sqrt{4D_r t}} &= c_s \\ C_3 \operatorname{erf} c\frac{s(t)}{\sqrt{4D_g t}} &= c_s \end{aligned} \tag{16}$$

Application of the continuity flux condition leads to

$$\sqrt{D_r} C_2 e^{\frac{-\xi^2}{4D_r}} = -\sqrt{D_g} C_3 e^{\frac{-\xi^2}{4D_g}} \tag{17}$$

where $\xi = s(t) / \sqrt{t}$.
Combinations of Eqs. (16) and (17) leads to

$$\frac{c_s}{c_0 - c_s}\sqrt{\frac{D_g}{D_r}} = \psi(k) \quad , \tag{18a}$$

where

$$\psi(k) = e^{\frac{\xi^2}{4}\left(\frac{1}{D_g}-\frac{1}{D_r}\right)} \frac{erfc\left(\frac{\xi}{\sqrt{4D_g}}\right)}{erf\left(\frac{\xi}{\sqrt{4D_r}}\right)} \tag{18b}$$

It follows immediately that ξ is a constant for a given value c_s, meaning that the the boundary $s(t)$ moves proportional to the square root of t. Note that $\psi(k=0)=\infty$, and $\psi(k\to\infty)$ tends to zero. Differentiation of (18b) with MAPLE shows that $d\psi(k)/dk < 0$. Moreover, $c_s / (c_0 - c_s)$ monotonically increases from 0 when $c_s = 0$ to ∞ when $c_s = c_0$. Therefore Eq. (18) has always one and only one solution.
Computations show that for $D_g < D_r$ the interface position $s(t)$ moves faster than for $D_g = D_r$. This paradox can be explained by a mass balance consideration. Less penetrant will move beyond the interface if $D_g < D_r$ (see Fig. 2) whereas the penetrant influx at $x=0$ is determined by the product of the concentration gradient and D_r. Therefore more mass will accumulate upstream of the interface $s(t)$.

Laplace solution of linearized equation

It is insightful to solve a linearized form of Eq. (13), i.e.,

$$\phi = \phi^{(0)} + \omega,$$

where ω is small. In this case a non-zero initial concentration $\phi^{(0)}<\phi_c$ is considered. Retaining only first order terms leads to

$$\begin{aligned} \frac{\partial \omega}{\partial t} &= \frac{\partial}{\partial x}\left(D_g \frac{\partial \omega}{\partial x}\right) + \frac{1}{B}\frac{\partial}{\partial x} \\ &\left(D_g \phi^{(0)} \frac{\partial}{\partial x}\left(\exp\left(-m\phi^{(0)}\right)\frac{\partial \omega}{\partial t}\right)\right). \end{aligned} \tag{18}$$

Consider a boundary concentration $\phi^{(b)}$.

Laplace transformation leads to (assuming a constant diffusion coefficient, $\phi < \phi_c$)

$$s\hat{\omega} = D_g\left(\frac{\phi^{(0)} s\, e^{\left(-m\phi^{(0)}\right)}}{B} + 1\right)\frac{\partial^2 \hat{\omega}}{\partial x^2} =: \left(\Lambda s + D_g\right)\frac{\partial^2 \hat{\omega}}{\partial x^2}.$$

The solution is

$$\hat{\omega} = L\left(\phi^{(b)} - \phi^{(0)}\right)\exp\left(-\sqrt{\frac{s}{\Lambda s + D_g}}x\right),$$

where L(f) denotes the Laplace transform of f. If $\phi^{(b)}$ were independent of time L $(\phi^{(b)} - \phi^{(0)}) = (\phi^{(b)} - \phi^{(0)})/s$.

Parameter	
D_g	10^{-11} m^2/s
D_r	10^{-10} m^2/s
M	10-30
Ω	1.68 x 10^{-29} m^3/molecule
η_0	10^{15} Ns/m^2
Φ_0	0.205
Φ_c	0.10 x Φ_0
Length	10^{-2} m
T	45°C

Table 1 Parameters used in simulation for a CO_2–coal system.

If $\phi^{(b)} = \phi_\infty^{(b)}(1-e^{-t/\tau})$, L $(\phi^{(b)} - \phi^{(0)}) = (\phi_\infty^{(b)} - \phi^{(0)})/s - \phi_\infty^{(b)}/(s+1/\tau)$.
Note that if $\phi^{(b)}$ were independent of time would lead for short times (large s) that ω is independent of time.

$$\omega = \left(\phi^{(b)} - \phi^{(0)}\right)\exp\left(-\sqrt{\frac{1}{\Lambda}}x\right) \tag{19}$$

For long times, i.e. for s is small, the solution reverts to pure diffusion behavior, i.e.,

$$\omega = \left(\phi^{(b)} - \phi^{(0)}\right) erfc\left(-\frac{x}{2\sqrt{D_g t}}\right) . \tag{20}$$

Also still assuming that $\phi^{(b)}$ is independent of time leads for the cumulative flux into the slab at x= 0 to

$$\widehat{F}(s) = \left(\phi^{(b)} - \phi^{(0)}\right)\sqrt{\frac{\Lambda s + D_g}{s^3}} \quad . \qquad (21)$$

The cumulative flux will be constant at early times (s→ ∞), because $\widehat{F}(s) \sim 1/s$. This indicates that the surface saturation process (Eq. (12)) determines the cumulative flux. The linearized profile, which would be obtained as an instantaneous response to the surface volume fraction, can be discerned in Fig. 2 as the horizontal part followed by the diffusion part in the curve ($\tau = 10^{-4}$).

At long times a pure diffusion flux is found, i.e.,

$$F(t) = 2\left(\phi^{(b)} - \phi^{(0)}\right)\sqrt{\frac{D_g t}{\pi}} \quad . \qquad (22)$$

Steady-state solution

Hui et al. (1987a, 1987b) suggest that Eq. (13) can have approximately a traveling wave like solution if the diffusion coefficient in the glass state (initial coal) approaches zero.

The approximation would be valid for the intermediate time regime. This means that the velocity of the volume fraction ϕ_c at which the transition between the glass state and the rubber state occurs, is initially proportional to time. The computational results (below) that include the surface delay effects proposed by Hui et al. together with the analysis of the model equations show that such a steady state does not occur.

Computational results

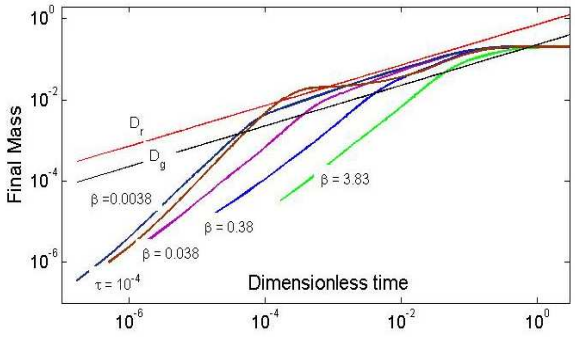

Fig. 2 Cumulative adsorbed mass (see appendix) for various values of the dimensionless parameter β [0.00383-3.83] with the material parameter m = 10. All other parameters are as in the table. Finally the process is governed by diffusion in rubbery coal until the particle gets saturated at ϕ_0 = 0.205. The straight lines D_r, D_g show pure Fickian diffusion. The line $\tau = 10^{-4}$ shows the behavior if the surface saturation were not given by Eq. (12), but by $\phi_0 (1-e^{-t/\tau})$.

The appendix derives the Finite Element representation of Eq. (13)**.** The initial conditions are that $\phi(x)$ and $\partial\phi/\partial t(x)$ are zero. The flux is zero at the end of the slab $(x = L)$ and therefore $(\partial\phi/\partial x)(L) = 0$. At $x = 0$, it is possible to obtain the volume fraction $\phi(x = 0)$ from Eq. (12). The parameters used for the simulation are summarized in Table **1**.

At early times the process is dominated by the slow saturation of the coal surface with the penetrant molecule. This process is described by Eq. (12).

Fig. 2 shows the cumulative adsorbed mass for various values of the dimensionless parameter β [0.00383-3.83] with the material parameter m = 10. The ratio between the diffusion coefficient in the rubber state and glass state D_r / D_g = 10. The two straight lines indicate the behavior of purely diffusional behavior with a glass and rubber diffusion coefficient respectively. In all cases the cumulative mass uptake tends to a long term diffusion process with a single rubber diffusion coefficient before the equilibrium saturation is attained. The curve in Fig. 2 that exceeds this long time behavior in part of the curve does not use Eq. (12) for the saturation of the coal surface but a faster process (1-exp(-t/τ)), with $\tau = 10^{-4}$ with β = 0.0383. The horizontal part of this curve shows the behavior derived in Eq. (19).

The effect of the material constant is very small, and is thus not shown as a separate curve in Fig. 2. Also changing the value of ϕ_c has a small effect on the results. In summary in the log-log plot the slope is always higher than 0.5, the value for Fickian diffusion, before the particle tends to the equilibrium saturation.

It appears that the term super-diffusion is sometimes misleading. If initially surface saturation effects occur the cumulative mass uptake in a log-log plot appears faster than the diffusional square root behavior, but the mass uptake is slower than for a single diffusion process with a rubber like diffusion coefficient. Such a behavior would also occur when there are two diffusion cofficients (Siemons et al. 2004), without a term describing stress-induced diffusion. If the surface saturation effects were absent (Thomas and Windle 1982) then indeed stress induced diffusion would lead to a mass uptake that can be faster than ordinary diffusion (see curve $\tau = 10^{-4}$ in Fig. 2). However after its initial increase, this case leads to a plateau with a slope much less than 0.5.

The cumulative sorption rates give similar behavior as the Rückenstein model (Rückenstein 1971, Shi and Durucan 2003, Siemons et al. 2004). The advantage of the T&W model, however, is that it can also calculate (see Eq. (5)) the resulting coal swelling effects.

Conclusions

- There is a large body of literature that supports analogy between CO_2 uptake in coal and the diffusion of a penetrant (e.g., CO_2) in polymers. The T&W model, which has been rederived by Hui et al. (1987a, 1987b) is used to describe the penetrant diffusion influenced by induced stress effects.
- A dimensional analysis shows that the relaxation dependent term in the model equation becomes relatively smaller as the penetrant (CO_2) intrudes further in the coal.

- A model, originally proposed by Sherwood and Pigford, can be adapted to show that - in the absence of relaxation, but in the presence of the contrast in diffusion coefficients - the penetration rate will be proportional to the square root of time.
- Solution of the T&W model equation in linearized form, i.e., in the absence of diffusion contrast shows the salient features of the stress induced diffusion, viz. a period dominated by saturating the surface, an intermediate regime where there is case II diffusion, and a long time phase, where the solution reverts to ordinary diffusion. The version of the T&W model derived by Hui does not show this behavior exceeding Fickian diffusion due to the slow saturation of the surface exposed to the penetrant (CO_2).
- Numerical results obtained with an inhouse developed FEM code shows that "Super-diffusion", i.e., that the penetration rate is faster than $t^{\frac{1}{2}}$, occurs only in the initial stages of the process when the surface gets saturated according to Eq. (12). For the surface saturation process, the term superdiffusion is misleading as the cumulative mass uptake is always less than for the Sherwood & Pigford model, which disregards stress effects.
- The cumulative sorption rates give similar behavior as the Rückenstein model. The advantage of the T&W model, however, is that it can also be used to calculate (see Eq. (5)) the resulting coal swelling effects.

Symbols

$B = k_B T / \Omega \eta_o$,
$c =$ *volume fraction in Sherwood –Pigford model [-],*
$c_o =$ *volume fraction at z=0 [-],*
$c_s =$ *volume fraction at s(t) [-],*
$D_g =$ *diffusion coefficient characteristic of a glassy coal [m^2/s],*
$D_r =$ *diffusion coefficient characteristic of a swollen (rubbery) coal [m^2/s],* $D_e =$ *Deborah number [-],*
$J =$ *volumetric flux [m/s],*
$k,\ k_1,\ k_2 =$ *constants incorporating characteristics of the macromolecular network system and the penetrant [-],*
$k_B =$ *Boltzmann constant [1.37983 x 10^{-23} J/molecule/K]],*
$l =$ *penetration depth [* m *],*
$L =$ *characteristic length [m],*
$m =$ *material constant [-],*
$M_t =$ *dimensionless mass uptake [-],*
$M_e =$ *equilibrium mass uptake [-],*
$n =$ *diffusional exponent [-],*
$P_{xx} =$ *viscous stress [kg/m^2],*
$T =$ *temperature [K],*
$z =$ *distance in Sherwood-Pigford model [m],*
$s(t) =$ *distance at which c=c$_s$ [m],*

$$\beta = \frac{\Omega D_g \eta_0}{k_B T L^2}$$

$\varepsilon =$ *small number [~],*
$\eta_l =$ *elongational viscosity of coal [Ns/m^2],*
$\eta_0 =$ *volumetric viscosity of the unswollen coal sample [Ns/m^2],*
$\theta =$ *characteristic diffusion time [* s *],*
$\lambda =$ *characteristic time for the macromolecular penetrant system [s],*
$\Lambda =$ *parameter in linear model [m^2],*
$\mu =$ *chemical potential [J/molecule],*
$\phi^{(0)} =$ *initial volume fraction in linear model [-],*
$\phi^{(b)} =$ *boundary volume fraction in linear model [-],*
$\phi =$ *volume fraction of the penetrant [-],*
$\phi_o =$ *equilibrium volume fraction [-],*
$\phi_c =$ *critical volume fraction [-],*
$\xi\sqrt{t} =$ *penetration rate in Sherwood-Pigford model,*
$\omega =$ *volume fraction deviation in linear model [-],*
$\Omega =$ *partial molar volume of CO$_2$ [m^3/molecule].*

Acknowledgements

This work was funded by the CO_2 sequestration project "RECOPOL", the Dutch "CATO" and the "NWO-NOVEM" programme. At the very onset, we would like to thank Prof. Harpalani from the University of Southern Illinois, Carbondale and Prof. Dan Marchesin from IMPA, Rio de Janeiro, Brazil for their valuable input. EC support by Marie Curie project No 35868, Greenhouse-gas Removal Apprenticeship and Student Program (GRASP), is acknowledged. Illuminating discussions with Dr. K.H.A.A. Wolf have greatly contributed to this paper. The paper also benefited from numerous discussions in workshops organized by the NUPUS collaboration project between the University of Stuttgart and Dutch Universities.

References

Alfrey, E.F. Gurnee and W.G. Lloyd, Diffusion in glassy polymers, *Journal of Polymer Science* Part **C 12**, pp. 249–261 (1966).

Argon, A.S., Cohen, R.E., and Patel, A.C. A mechanistic model of case II diffusion of a diluent into a glassy polymer, *Polymer*, **40**, 6991–7012 (1999a).

Barbara D. Barr-Howell, John M. Howell,' and Nikolaos A. Peppas, "Transport of Penetrants in the Macromolecular Structure of Coals. 6. Amine Transport Mechanisms", *Energy & Fuels*, Vol. **1**, No. 2, 181-186 (1987).

Battistutta, E. Hemert, P. van, Wolf, K.H., and Bruining, H. "Comparison of sorption behavior of CH_4 and the main flue gas components CO_2 and N_2", Submitted to the *International Journal of Coal Geology* (2009).

Bird, R.B., Stewart, W.E. and Lightfoot, E.N.: "Transport Phenomena", 2nd edition, John Wiley & Sons, Inc. New York (2002).

Brenner, D, "The macromolecular nature of bituminous coal", *Fuel*, Vol **64**, 167-173 (1985).

Brenner, D., "The macromolecular states of solvent-swollen and dry coal", *Nature* **306**, 772 - 773 (22 December (1983).

Cody, G.D., Davis, A. and Hatcher, P. G., "The dynamic nature of coal's macromolecuklar structure: viscoelastic analysis of solvent-swollen coals", *Energy&Fuels*, Vol **7**, No 4, 463-468 (1993).

Durning, C.: "Differential sorption in viscoelastic-fluids", *Journal of Polymer Science: Polymer Physics Edition*, **23** (9) 1831--1855 (1985).

Gall, T.P. et al.: "Diffusion of deuterated toluene in polystyrene", *Polymer* **32**, 265-271 (1991).

Govindjee, S. and Simo, J.C., Coupled stress-diffusion: Case II. *J. Mech. Phys. Solids* **341**, pp. 863–887 (1993).

Goodman, A.L, R.N. Favors, and John W. Larsen, "Argonne Coal Structure Rearrangement Caused by Sorption of CO_2", *Energy and Fuels*, Vol **20**, No 6, 2537-2543 (2006).

Hsieh and Duda, S.T. Hsieh and L.J. Duda, Probing coal structure with organic vapour sorption. *Fuel* **66** (1987), pp. 170–178 (1987).

Hui, C.-Y., Wu, K.-C., Lasky, R.C. and Kramer, E.J., Case-II diffusion in polymers. I. Transient swelling. *Journal of Applied Physics* **61**, pp. 5129–5136 (1987).

Hui, C.-Y., Wu, K.-C., Lasky, R.C. and Kramer, E.J., Case-II diffusion in polymers. II. Steady-state front motion. *Journal of Applied Physics* **61**, pp. 5137–5149 (1987).

Jou, D., Casas-Vazquez, J., Lebon, G. : "Extended Irreversible Thermodynamics", Springer-Verlag, Heidelberg (2001).

Karacan, C.Z., "Heterogeneous Sorption and Swelling in a Confined and Stresses Coal During CO_2 injection", *Energy & Fuels*, Vol. **17**, No. 6, 1595-1608 (2003).

Krzesińska, M., Averaged Structural Units in Bituminous Coals Studied by Means of Ultrasonc Wave Velocity Measurements", *Energy and Fuels* Vol **15** No 4, 930-935 (2001).

Landau, L.D., Lifshitz, E. M.: "Fluid Mechanics", Pergamon Press. Oxford (1975).

Lasky, R.C. et al.: "The initial stages of Case II diffusion at low penetrant activities", *Polymer* **29**, 673-679 (1988).

Marta Krzesińska, Effect of Solvents Treatment on the Elastic Properties of Bituminous Coal", *Energy and Fuels* Vol **15**, No 2, 324-330 (2001).

Mazumder, S., and K.H. Wolf, Differential swelling and permeability change of coal in response to CO2 injection for ECBM: *International Journal of Coal Geology*, v. **74**, p. 123-138, (2008).

Mikelic, A., and Bruining, J., Analysis of model equations for stress-enhanced diffusion in coal layers. Part I: Existence of a weak solution, *SIAM J. Math. Anal.* Volume **40**, Issue 4, pp. 1671-1691 (2008).

Mojtaba Mirzaeian and Peter J. Hall, "The interactions of coal with CO_2 and its effect on Coal Structure, *Energy & Fuels*, Vol. **20**, No. 5, 2022-2027 (2006).

Pagnier H, van Bergen F. Field experiment of CO_2 emission reduction by means of CO2 storage in coal seams in the Silesian Coal Basin of Poland (RECOPOL). In: Gale JJ, Kaya Y, editors. Proceedings of the 6th International Conference on Greenhouse Gas Control Technologies. Oxford, UK: Elsevier; (2003).

Ritger, P. L. and Peppas, N.A., "Transport of penetrants in the macromolecular structure of coals, 4. Models for analysis of dynamic penetrant transport", *Fuel* 66, 815-826 (1987-a).

Ritger, P. L. and Peppas, N.A., "Transport of penetrants in the macromolecular structure of coals, 7. Transport in thin coal sections", *Fuel* 66, 1379-1388 (1987-b).

Rückenstein, E., Vaidyanathan, A.S., and Youngquist, G.R., Sorption by Solids with Bidisperse Pore Structures. *Chemical Engineering Sciences*, **26**: 1305-1318 (1971).

Siemons, N., Wolf, K.H., and Bruining, J., "Interpretation of Carbon Dioxide Diffusion Behavior in Coals", *International Journal of Coal Geology*, **72**, (3-4), pp 315-324 (2007).

Siemons, N., Bruining, H. and Krooss, B.M., Upscaled diffusion in coal particles, *Geologica Belgica* - Volume **7** (3-4) 12 pages (2004).

Shi, J.Q. and Durucan, S., Drawdown Induced Changes in Permeability of Coalbeds: A New Interpretation of the Reservoir Response to Primary Recovery, *Transport in Porous Media* **56:** 1–16, 2004.

Shi, J.Q. and Durucan, S., A bidisperse pore diffusion model for methane displacement desorption in coal by CO2 injection, *Fuel* **82**, 1219–1229 (2003).

Stanislaw Nagy, Use of carbon dioxide in underground natural gas storage processes, *Acta Montanistica Slovaca* Ročník **11**, mimoriadne číslo 1, 116-119, (2006).

Thomas, N.L and Windle, A.H., A theory of case II diffusion, *Polymer* **23,** 529--542 (1982).

Vrentas, J.S., Jarzebski, C.M and Duda, J.L., A Deborah number for diffusion in polymer-solvent systems. *AIChE J.* **21**, p. 894-901, (1975).

Vrentas, J.S. and Duda, J.L., Diffusion in polymer-solvent systems. III. Construction of Deborah number diagrams. *J. Polym. Sci. Polym. Phys*. Ed. **15**, pp. 441–453 (1977).

Appendix 1: Numerical Solution method

Here the numerical model is formulated for the partial differential equation with boundary and initial conditions. The purpose is that a research oriented reader can develop or modify a computer programme for comparison to experimental results. The programme uses a 2-D or 3-D representation of the following partial differential equation with boundary and initial conditions

$$\begin{aligned}
&\frac{\partial\phi}{\partial t} - \nabla\bullet\left(D(\phi)\nabla\phi + \frac{D(\phi)}{B}\nabla\left(e^{-m\phi}\frac{\partial\phi}{\partial t}\right)\right) = 0 \quad \text{for } \mathbf{x}\in\Omega,\ t>0\\
&D(\phi)\frac{\partial\phi}{\partial n} + \frac{D(\phi)}{B}\frac{\partial}{\partial n}\left(e^{-m\phi}\frac{\partial\phi}{\partial t}\right) = 0 \qquad \text{for } \mathbf{x}\in\partial\Omega_N,\ t>0\\
&\phi(\mathbf{x},t) = \psi(t) \qquad \text{for } \mathbf{x}\in\partial\Omega_E,\ t>0\\
&\phi(\mathbf{x},0) = 0 \qquad \text{for } \mathbf{x}\in\Omega
\end{aligned} \tag{1}$$

Here Ω denotes the (Lipschitz) domain of computation, $\partial\Omega_N$ and $\partial\Omega_E$ denote disjoint parts of the boundary of Ω, such that $\partial\Omega_E \cup \partial\Omega_N$ gives the entire boundary of the domain of computation. The function $\psi(t)$ defines the essential boundary condition in the following implicit way.

$$t = -\phi_0\frac{\eta_0\Omega}{k_BT}\int_0^{\frac{\psi}{\psi_0}}\frac{e^{-m\psi_0 s}}{\ln(s)}ds\ , \tag{2}$$

where here Ω means the molecular volume. It is shown in ref. 17 that the integral in (Eq. 2) exists for $0<\psi<\psi_0$. The solution of the problem is obtained by a Finite Element Method. To that extent, the partial differential equation is multiplied by a testfunction, which satisfies $v=v(\mathbf{x})=0$ on $\partial\Omega_E$. Subsequently, integration over the domain Ω is carried out. This gives the following Finite Element formulation:

Find ϕ, subject to $\phi(\mathbf{x},t=0)=0$ on Ω and $\phi(\mathbf{x},t)=\psi(t)$ on $\partial\Omega_E$, such that

$$\int_\Omega \frac{\partial\phi}{\partial t}v d\Omega - \int_\Omega \nabla\bullet\left(D(\phi)\nabla\phi + \frac{D(\phi)}{B}\nabla\left(e^{-m\phi}\frac{\partial\phi}{\partial t}\right)\right)v d\Omega = 0 \tag{3}$$

for all $\mathbf{v(x)}$, subject to $\mathbf{v(x)}=0$ on $\partial\Omega_E$.

For ϕ to be a solution, it is necessary that the above integrals exist (ref 17) at each time t. A semi-implicit time integration is used, in which all nonlinearities are computed at the previous timestep, it is convenient to cast the above expression into the form of a parabolic heat equation. To accomplish this form, the Product Rule for differentiation is applied on the third term of equation (4). Some rearrangement leads to

$$\int_{\Omega}\left(\frac{\partial\phi}{\partial t}v+\frac{D(\phi)}{B}e^{-m\phi}\left(\nabla\left(\frac{\partial\phi}{\partial t}\right)-m\frac{\partial\phi}{\partial t}\nabla\phi\right)\bullet\nabla v\right)d\Omega + \int_{\Omega}D(\phi)\nabla\phi\bullet\nabla v\ \mathrm{d}\Omega\ =0 \quad . \quad (4)$$

To solve equation (4), the computational domain Ω is divided into *m* triangular elements or tetrahedral elements τ_p in $\mathbb{R}^2$ and $\mathbb{R}^3$, such that $\cup_{p=1}^{m}\overline{\tau}_p=\Omega_h$, where Ω_h is the polygonal representation of Ω with the elements, such that $\Omega_h\rightarrow\Omega$ as $m\rightarrow\infty$. Conforming linear elements are considered, so the vertices of the elements are the meshpoints of the domain of computation. Each meshpoint, x_i corresponds to a basis function v_i (**x**) such that

$$v_j(\mathbf{x}_i)=\delta_{ij}=\begin{cases}1, & \mathrm{j}=i\\ 0, & \text{else}\end{cases} \quad (5)$$

To deal with the Dirichlet boundary condition, see equation (1) and (2), an adaptive time stepping is implemented, defined by

$$\Delta t^{k+1}=-\phi_0\frac{\eta_0\Omega}{k_BT}\int_{\frac{\psi^k}{\psi_0}}^{\frac{\psi^{k+1}}{\psi_0}}\frac{e^{-m\psi_0 s}}{\ln(s)}ds \quad (6)$$

until the surface is almost completely saturated, before it reverts to a conventional time stepping scheme.

Here k denotes the time step with equidistant points $\psi^k=k\Delta\psi$ such that $\psi^K=\psi_0$. The Trapezoidal Rule is used to approximate the above integral. For all $k\geq K$, $\Delta t^k=\Delta t^K$. The numerical solution, ϕ_h (**x**,t), is written as

$$\phi_h(\mathbf{x},t)=\sum_{j=1}^{n}\phi_j(t)v_j(\mathbf{x})+\psi(t)\sum_{j=n+1}^{n+n_D}v_j(\mathbf{x}), \quad (7)$$

with n_D nodal points on $\partial\Omega_E$. A semi-implicit time integration (IMplicit EXplicit) method is implemented leading to

$$M\left(\phi_h^k\right)\underline{\phi}^{k+1}=M\left(\phi_h^k\right)\underline{\phi}^k+\Delta t^{k+1}S\left(\phi_h^{k+1}\right)\underline{\phi}^{k+1}+\underline{f}^{k+1},$$

where $\underline{\phi}^k=[\phi_h(\mathbf{x}_1,t)\ldots\phi_h(\mathbf{x}_n,t)]^T$. Here, the mass- and stiffness matrices M and S and righthand side vector $\underline{f}$ are defined by

$$M_{ij}\left(\phi_h^k\right)=\int_{\Omega_h}v_iv_j+\frac{D\left(\phi_h^k\right)}{B}e^{-m\phi_h^k}\left(\nabla v_i\bullet\nabla v_j-mv_j\nabla\phi_h^k\bullet\nabla v_i\right)d\Omega,$$

$$S_{ij}\left(\phi_h^k\right)=\int_{\Omega_h}D\left(\phi_h^k\right)\nabla v_i\bullet\nabla v_j d\Omega,$$

$$f_i\left(\phi_h^k\right)=\sum_{j=n+1}^{n+n_D}\frac{\psi^{k+1}-\psi^k}{\Delta t^{k+1}}\times \times\int_{\Omega_h}v_iv_j+\frac{D\left(\phi_h^k\right)}{B}e^{-m\phi_h^k}\left(\nabla v_i\bullet\nabla v_j-mv_j\nabla\phi_h^k\bullet\nabla v_i\right)d\Omega+ +\int_{\Omega_h}D\left(\phi_h^k\right)\nabla v_i\bullet\nabla v_j d\Omega$$

For convenience, the matrices are obtained by an elementwise assembly procedure over the element matrices. The element matrices are computed by the use of Newton-Cotes numerical integration.